Chapter

Functionalized MCM-48 as Carrier for In Vitro Controlled Release of an Active Biomolecule, L-Arginine

Anjali Uday Patel and Priyanka Dipakbhai Solanki

Abstract

The present chapter describes the synthesis, characterizations, and application of MCM-48 functionalized by an inorganic moiety, as a carrier. MCM-48 functionalized by 12-tungstophophoric acid (TPA) (TPA-MCM-48) and L-arginine was loaded into pure as well as functionalized MCM-48. Both the materials were characterized by various physicochemical techniques and evaluated for in vitro release of L-arginine at body temperature under different conditions. A study on release kinetics was carried out using first-order release kinetic model, while the mechanism were by Higuchi model. Further, to see the influence of TPA on release rate, release profile obtained from pure and functionalized MCM-48 was compared.

Keywords: MCM-48, 12-tungstophosphoric acid, L-arginine, in vitro release, kinetics and mechanism

1. Introduction

A semi essential amino acid, L-arginine is the main source of generation of NO via NO synthase (NOS), nitric oxide (NO), polyamines and agmatine, which also influence hormonal release and the synthesis of pyrimidine bases [1–4]. The three NOS isoforms have been found to be expressed in the kidney [4]. In the kidney endothelial NOS is important in the maintenance of glomerular filtration rate, regional vascular tone, and renal blood flow. The neuronal NOS (nNOS) is expressed primarily in the macula densa and participates in the control of glomerular hemodynamic via tubuloglomerular feedback and rennin release. The inducible (iNOS) is expressed in the kidney under pathological condition in the glomerular mesangium, infiltrating macrophages and tubules [5]. L-arginine is the substrate for arginases, a group of enzyme that are involved in tissue repair processes and that metabolize L-arginine to l-ornithine [6] as well as precursor for polyamine synthesis which is also involved in tissue repair and wound healing [7, 8]. During the time of stress, body does not provide sufficient amount of L-arginine for metabolic needs. Hence, under this condition, L-arginine supplementation has been considered as an adjunct treatment for restoring normal function [7, 9, 10]. It was also found that compared to oral administration, intravenous administration of L-arginine to the patients with coronary artery disease increases

the bioavailability of vascular nitric oxide (NO) which shows the vasodilator effect. Further, it was found that in case of oral administration, the bio-availability of L-arginine decreases as it is utilized by arginase for the production of urea and ornithine and thus competes with NO synthase for substrate availability [1, 11], 40% L-arginine is degraded in the intestine by arginase [12]. The mentioned problem can be overcome if some carrier will be used. The advantage of using carrier is expected to provide sufficient amount of L-arginine for NO production as the carrier can effectively load the desired amount of L-arginine as well as release it in control manner.

Thus, even though, L-arginine is important and is used as drug under certain conditions, no work has been found on controlled release of L-arginine except one which deals with the adsorption of L-arginine on SBA-15 at different pH by Deng et al. [13].

As M41S family have properties like higher surface area, ordered porosity, higher adsorption capacity, biocompatibility and non-cytotoxicity, they have been effectively explored as drug delivery carrier [14] and a number of reports are available on unfunctionalized or functionalized MCM-41/SBA-15 [15–40]. At the same time, very few reports are available on MCM-48, another important member of the M41S family as drug delivery carrier [40–43]. Arruebo et al. have reported iron loaded MCM-48 as drug delivery carrier [40]. Yang et al. have reported functionalization of MCM-48 by hydroxyapatite and used as a carrier for captopril [41]. Gai et al. have reported in vitro release of captopril using MCM-48 functionalized by VO4:Eu3+ [42]. Aghaei et al. have reported in vitro release of ibuprofen using MCM-48 functionalized by hydroxyapatite [43]. Recently, Popat et al. have reported the release profile of Sulfasalazine from MCM-48. [44]. Choi et al. have reported the comparative study for release of hydrophilic dye (Rose bengal) and hydrophobic molecule [Camptothecin (CPT) and Rhodamine 6G (R6G)] from MCM-48 [45]. Berger et al. have reported comparative study for release of aminoglycoside from MCM-48 [39].

A literature survey shows that MCM-48 has been used as a carrier either in pure form or in functionalized form using organic moiety [41, 44, 46] and no reports are available on functionalization of MCM−48 by inorganic moiety.

In this regard, polyoxometalates (POMs), early transition metal oxygen anion clusters with metal in their higher oxidation states, are excellent candidates for the same as they have already been used in medicinal chemistry. The most investigated POMs are the Keggin type, represented by the general formula $[Xn^{n+}M_{12}O_{40}]^{(8-n)-}$, where Xn^{n+} is a central heteroatom (Si^{4+}, P^{5+}, etc.) and M is an addenda atom (W^{6+}, Mo^{6+}, V^{5+}, etc.). They have large number of water molecules and terminal oxygen atoms through which they can bind to the different functional groups of drug molecules. Literature survey shows that amongst all Keggin POMs, 12-tungstophosphoric acid (TPA) has been widely used in medicinal chemistry [47–51]. In the present chapter, first time we are describing the use of 12-tungstophosphoric acid (TPA) for functionalization of MCM-48.

The present chapter describes synthesis of MCM-48, its functionalization by TPA (TPA-MCM-48) and encapsulation of L-arginine into TPA-MCM-48 ($L\text{-}arg_1$/TPA-MCM-48) as well as their characterization using various physicochemical techniques. In vitro release of L-arginine was carried out at body temperature under static and dynamic condition and different pH. L-arginine release kinetics and mechanism was also investigated using first order release kinetic model and Higuchi model. Further, in order to see the influence of TPA on release rate, L-arginine was loaded on pure MCM-48 ($L\text{-}arg_1$/MCM-48) and its release study was carried out under same experimental condition.

2. Experimental

2.1 Materials

L-arginine (SRL), Tetraethyl Orthosilicate (TEOS), Cetyltrimethylammonum Bromide (CTAB), Ninhydrin, Sodium hydroxide (NaOH), 12-Tungstophosphoric acid (TPA) and Ethanol (absolute) were received from Merck. All the chemicals were of A.R. Grade and used without any further purification.

Simulated body fluid (SBF): NaCl (7.996 g), $NaHCO_3$ (0.350 g), KCl (0.224 g), $K_2HPO_4.3H_2O$ (0.22 g), $MgCl_2.6H_2O$ (0.305 g), 1 $molL^{-1}$ HCl (40 ml), $CaCl_2$ (0.278 g), Na_2SO_4 (0.071 g) and $NH_2C(CH_2OH)_3$ (6.057 g) were dissolved in small amount of water and then dilute to 1 L with distilled water [46, 52].

Simulated gastric fluid (SGF): 6.217 g of conc. HCl was place into 1 L volumetric flask and then diluted up to the mark using distilled water.

2.2 Synthesis of mesoporous MCM-48

The synthesis of MCM-48 was carried out as described in literature [53]. 2.4 g of CTAB was dissolved in 50 ml distilled water. To this clear solution of CTAB, 50 ml ethanol (0.87 mole) and 12.6 ml ammonia (32 wt%, 0.20 mole) were added. The mixture was then stirred for 10 min. After 10 min, 3.4 g TEOS (16 mole, 3.6 mL) was added to this homogeneous solution. The mixture was then stirred for 2 h. After stirring, the resulting white solid was filtered and wash with distilled water. The dried white material then calcined at 823 K for 6 h to remove the template. The resulting material was designated as MCM-48.

2.3 Synthesis of TPA functionalized MCM-48 (TPA-MCM-48)

MCM-48 was functionalized using TPA as functionalizing agent by incipient wet impregnation method [54]. 30% of TPA anchored to MCM-48 was synthesized. One g of MCM-48 was impregnated with an aqueous solution of TPA (0.3/30 g/mL of distilled water) and dried at 100°C for 10 h. The obtained material was designated as TPA-MCM-48.

2.4 Loading of L-arginine on TPA-MCM-48 and MCM-48

Loading of L-arginine was also carried out by incipient wet impregnation method where 1 g of TPA-MCM-48 and MCM-48 were impregnated with an aqueous solution of L-arginine (0.1 g/10 mL) and pH of the mixture was adjusted up to 4 using 0.1 M HCl solution and mixture was dried at 100°C for 5 h. The obtained material was designated as L-arg_1/TPA-MCM-48. Loading amount was also confirmed by thermal analysis which shows 0.1 g of L-arginine was loaded per g of both materials (TPA-MCM-48 and MCM-48). All the experiments were carried out three times for finding % errors with in data.

2.5 Preparation of calibration curve for determination of L-arginine

To obtained calibration curve of L-arginine, stock solution was prepared by dissolving 1 g of it in 100 ml SBF (1 mg/mL). Series of 25 mL Nessler's tubes containing 0.15–0.4 mL of this stock solution was diluted up to the 4 mL using distilled water. 1 mL of acetate buffer (pH 5.5) and 1 mL ninhydrin reagent (10% ninhydrin solution in ethanol) were added to diluted solutions. All the tubes were placed in

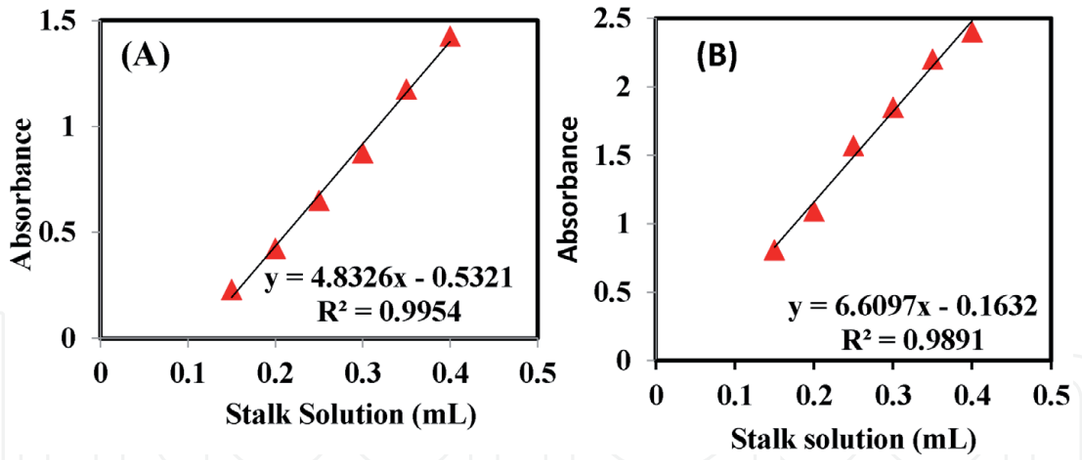

Figure 1.
Calibration curve of L-arginine in (A) SBF and (B) SGF.

boiling water bath up to 15 min for completion of reaction which was seen by the formation of purple color. The solutions were cooled under tap water, followed by addition of 1 mL of 50% ethanol and absorption was taken at 570 nm using Systronics UV–Visible-spectrophotometer. Similarly, calibration curve was obtained in SGF (**Figure 1**).

2.6 Characterization

The FTIR spectra of all materials were obtained by using KBr palate on Perkin Elmer instrument. TGA of the materials were carried out using a Mettler Toledo Star SW 7.01 instrument under nitrogen atmosphere from 30 to 570°C at the heating rate of 10°C/min. Adsorption–desorption isotherms of MCM-48, TPA-MCM-48 and L-arg$_1$/TPA-MCM-48 were recorded on a Micromeritics ASAP 2010 Surface area analyzer at liquid nitrogen temperature. From the adsorption desorption isotherms, specific surface area was calculated using BET method. The XRD pattern was obtained on PHILIPS PW-1830, with Cu Kα radiation (1.54 Å) and scanning angle from 0° to 10°. TEM analysis was carried out on JEOL (JAPAN) TEM instrument (model-JEM 100CX II) with accelerating voltage of 200 kV. The samples were dispersed in ethanol and ultrasonicated for 5–10 min. A small drop of the sample was then taken in a carbon coated copper grid and dried before viewing. ^{31}P MAS NMR spectra were recorded by BRUKER Avance DSX-300, at 121.49 MHz using a 7 mm rotor probe with 85% phosphoric acid as an external standard. The spinning rate was 5–7 kHz. Catalyst samples, after treatment were kept in a desiccator over P_2O_5 until the NMR measurement. The ^{29}Si NMR spectra were recorded at Mercury Plus 300 MHz using a 5 mm Dual Broad Band rotor probe with TMS as an external standard.

2.7 In vitro release study of L-arginine

In vitro release profile of L-arginine was obtained by soaking 0.5 g of L-arginine loaded materials in 62.5 mL of SBF (0.8 mg of L-arginine in 1 mL SBF) at temperature of 37°C with 200 rpm. At predetermined time interval, 0.5 mL of released fluid was taken and immediately equal amount of fresh SBF was added to maintain the constant volume. This release fluid was analyzed for L-arginine content by treating it with 10% ninhydrin solution at 570 nm using UV–Visible spectrophotometer (PerkinElmer). Same study was also carried under static condition as well as at different pH (pH 7.4 and pH 1.2). All the experiments were repeated three times.

3. Result and discussion

3.1 Material characterization

FTIR spectrum of MCM-48 shows a broad band around 1100 and 1165 cm^{-1} corresponding to asymmetric stretching of Si-O-Si (**Figure 2b**), the bands at 640 and 3448 cm^{-1} are corresponding to symmetric vibrations of Si-O-Si and stretching vibration Si-OH band, respectively, in good agreement with the reported one [55]. The presence of typical bands of TPA at 982 cm^{-1} corresponding to Vas vibration of W = O_d, and 897 cm^{-1} for stretching vibrations of W-O-W, in TPA-MCM-48 [56] suggest the primary structure of TPA is remain intact even after functionalization of MCM-48. The absence of vibration band at 1080 cm^{-1} (Vs stretching of P-O) of TPA may be due to superimposition on the bands of MCM-48. The FTIR spectrum of L-arginine shows bands around 3151, 1680, 1574 cm^{-1} corresponds to N–H stretching vibration, NH_2 in plan bending vibration and C=O stretching vibration [57]. FTIR spectrum of L-arg_1/TPA-MCM-48 (**Figure 2d**) shows entire bands corresponding to TPA-MCM-48 with lower intensity suggesting multiple adsorption of it into TPA-MCM-48 which is further confirmed by Nitrogen adsorption–desorption surface area analysis (**Figure 3** and **Table 1**). It shows some additional bands at 3183 cm^{-1} due to the N-H stretching, 1690 cm^{-1} due to NH_2 in plane bending vibration and 1552 cm^{-1} due to C=O stretching vibration. The observed Shifting in the bands correspond to C=O group and N-H group indicate the interaction of L-arginine to TPA-MCM-48 through these functional group.

TGA analysis of pure MCM-48, TPA-MCM-48 and L-arg_1/TPA-MCM-48 are shown in **Figure 3**. MCM-48 shows initial weight loss of 0.7% up to 100°C. This initial weight loss may be due to adsorption of physically adsorbed water molecules. After that, no further weight loss is observed.

TGA curve of TPA-MCM-48 shows initial weight loss of 10–13% up to 100°C which indicate presence of adsorbed water, while the Second weight loss of 1–2% between 200 and 300°C corresponds to the loss of water of crystallization of Keggin

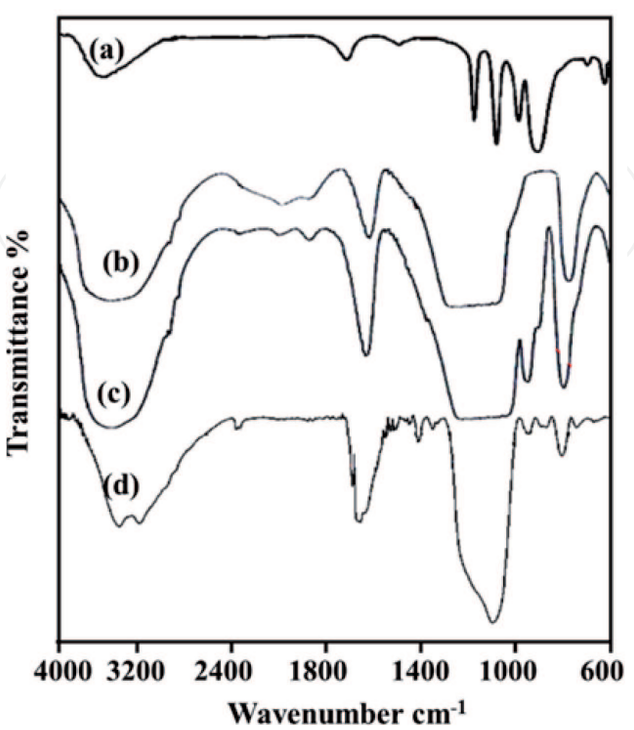

Figure 2.
FTIR spectra of (a) TPA, (b) MCM-48, (c) TPA-MCM-48 and (d) L-arg_1/TPA-MCM-48.

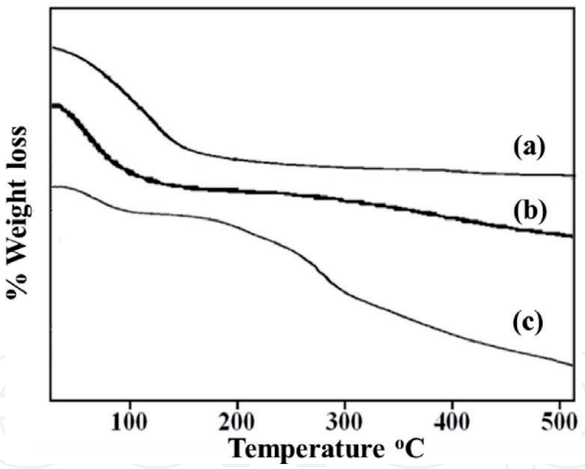

Figure 3.
TGA analysis (a) MCM-48, (b) TPA-MCM-48 and L-arg1/TPA-MCM-48.

Materials	Specific surface area (m2/g)	Pore volume (cm3/g)
MCM-48	1141	0.67
TPA-MCM-48	566	0.22 [R,S]
L-arg$_1$/TPA-MCM-48	68	0.10
L-arg1/MCM-48	109	0.25

Table 1.
Textural properties of MCM-48, TPA-MCM-48, L-arg1/TPA-MCM-48 and L-arg1/MCM-48.

ion. A gradual weight loss from 300 to 500°C was observed due to the difficulty in removal of water present in TPA molecules inside the channels of MCM-48. This types of inclusion can cause the stabilization of TPA molecules inside the channels of MCM-48.

TGA curve of L-arg$_1$/TPA-MCM-48 shows initial weight loss of 2.45% up to 100°C and further weight loss of 9.93% from 200 to 500°C. Initial weight loss may be due to the presence of adsorbed water. Weight loss from 200 to 490°C may be because of the removal of L-arginine from TPA-MCM-48.

Figure 4 shows nitrogen adsorption–desorption isotherm of MCM-48, TPA-MCM-48 and L-arg$_1$/TPA-MCM-48 and textural parameters are shown in **Table 1**. Isotherms of MCM-48 is type IV in nature and according to IUPAC classification it is the characteristic of mesoporous solids. This also suggests that functionalization as well as loading of L-arginine does not alter the structure of MCM-48 Decrease in surface area and pore volume is observed after functionalization of MCM-48 by TPA suggests the strong interaction of TPA with MCM-48. Further decrease in surface area and pore volume is observed in case of L-arg$_1$/TPA-MCM-48 which suggests the encapsulation of L-arginine into the mesoporous channel of TPA-MCM-48.

Figure 5 shows Low angle powder XRD of MCM-48, TPA-MCM-48 and L-arg$_1$/TPA-MCM-48. The XRD pattern of MCM-48 shows main characteristic peaks at 2.3° which indicates the presence of intact structure of MCM-48. It also shows broad shoulder at 3.0° corresponding to a plane 211 and 220, respectively. Several peaks in the range of 4–5° diffraction angles correspond to the reflections of 400, 321 and 420 planes of a typical MCM-48 meso-structure with Ia3d cubic symmetry. It is well known that the low angle XRD pattern are sensitive to pore filling and loaded materials show lowered intensity of characteristic peak compared to pure one. XRD

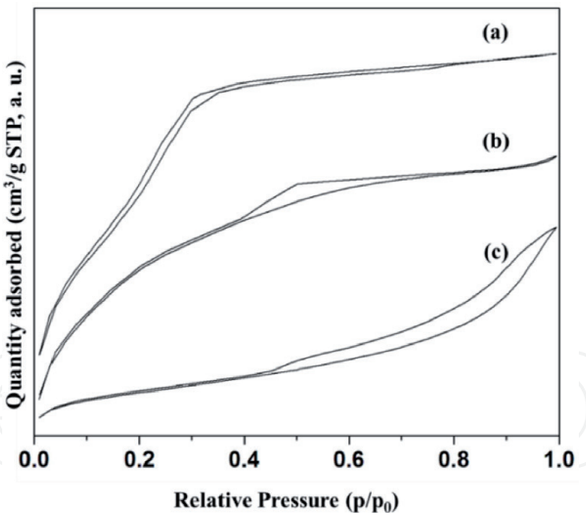

Figure 4.
Nitrogen adsorption–desorption isotherms of (a) MCM-48, (b) TPA-MCM-48 and (c) L-arg$_1$/TPA-MCM-48.

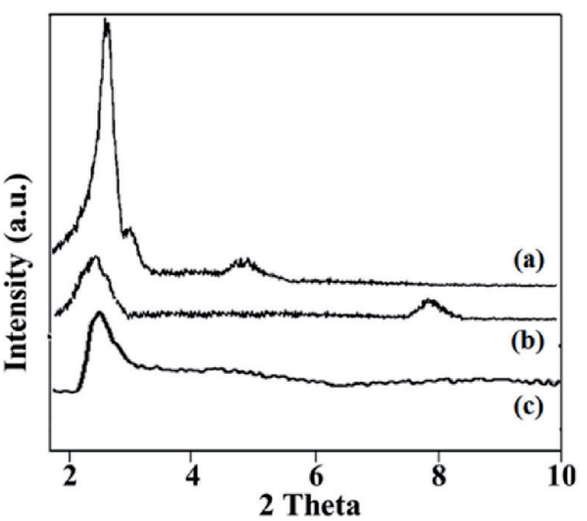

Figure 5.
Low angle powder XRD of (A) MCM-48, (B) TPA-MCM-48 and (C) L-arg$_1$/TPA-MCM-48.

pattern of TPA-MCM-48 and L-arg$_1$/TPA-MCM-48 shows characteristics peak at 2θ = 2.3° with lower intensity. Absence of any other peak indicates the insertion as well as homogeneous distribution of L-arginine into the mesoporous channels of TPA-MCM-48. In addition to this, disappearance of secondary peak at 2θ = 3–5° in case of L-arg$_1$/TPA-MCM-48 was observed. This is because further loading of L-arginine into functionalized MCM-48 may block the channels which have already been confirmed by BET analysis.

Figure 6 shows TEM images of MCM-48, TPA-MCM-48 and L-arg$_1$/TPA-MCM-48 at 50 nm resolution. The TEM image of MCM-48 shows very well ordered pore system with spherical morphology. It is well known in literature, that MCM-48 has a three dimensional pore system with two non-intersecting gyroidal pores. The TEM image of TPA-MCM-48 shows similar spherical morphology with porous system suggesting intact structure of MCM-48 even after functionalization. The TEM images of L-arg$_1$/TPA-MCM-48 also show spherical morphology and porous structure. Absence of any aggregation in TEM images of L-arg$_1$/TPA-MCM-48 suggests the homogeneous dispersion of L-arginine on TPA-MCM-48. Further the structure of TPA-MCM-48 remains intact even after loading of L-arginine.

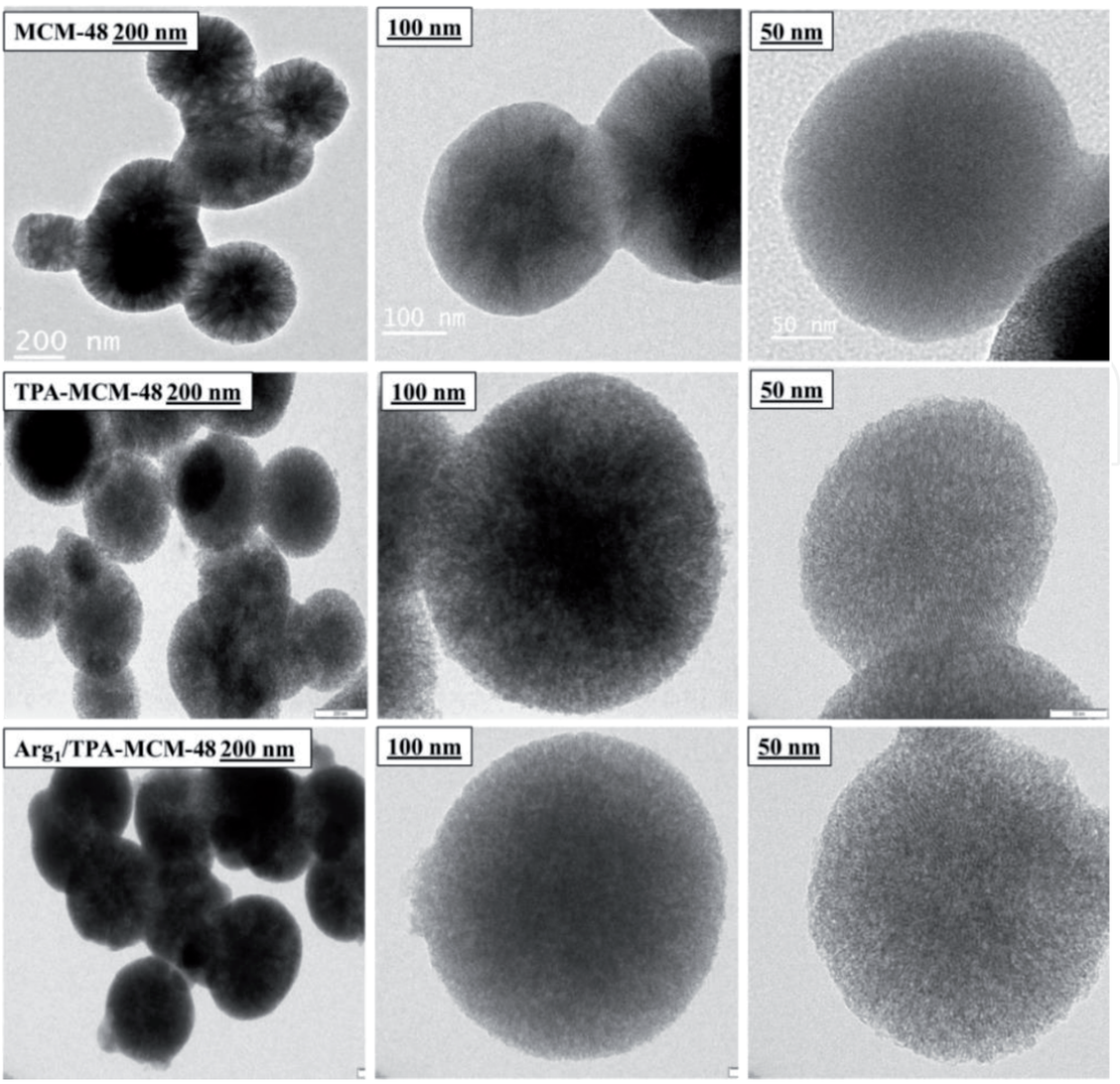

Figure 6.
TEM images of MCM-48, TPA-MCM-48 and L-arg$_1$/TPA-MCM-48 at 200, 100 and 50 nm resolution.

^{31}P MAS NMR is the most important method to study chemical environment around the phosphorous in heteropoly compounds. The ^{31}P MAS NMR spectra of TPA-MCM-48 and L-arg$_1$/TPA-MCM-48 are shown in **Figure 7**. The pure TPA shows single peak at −15.62 ppm and is in good agreement with the reported one [58]. The ^{31}P MAS NMR spectra of TPA-MCM-48 shows two peak at −12.27 and 3.060 ppm. The observed shift from −15.62 to −12.27 ppm is attributed to the strong interaction of MCM-48 with that of TPA as well as the presence of TPA inside the MCM-48. These results are in good agreement with reported one [59].

Further shift in this peak is observed from −12.27 to −9.24 ppm for L-arg$_1$/TPA-MCM-48 which also suggest the interaction of TPA with that of L-arginine which was further confirmed by ^{29}Si MAS NMR.

^{29}Si MAS NMR is a useful technique to study the chemical environment around the silicon nuclei in the mesoporous materials. **Figure 8** represents the ^{29}Si MAS NMR spectra of MCM-48, TPA-MCM-48 and L-arg$_1$/TPA-MCM-48. A broad peak of MCM-48 between −90 to −125 ppm observed which can be attributed to three main part of the peak with chemical shift at −92, −99 and − 108 ppm (**Figure 8a**, **Table 2**). These signals resulted from Q2 (−92 ppm), Q3 (−99 ppm) and Q4 (−108 ppm) silicon nuclei.

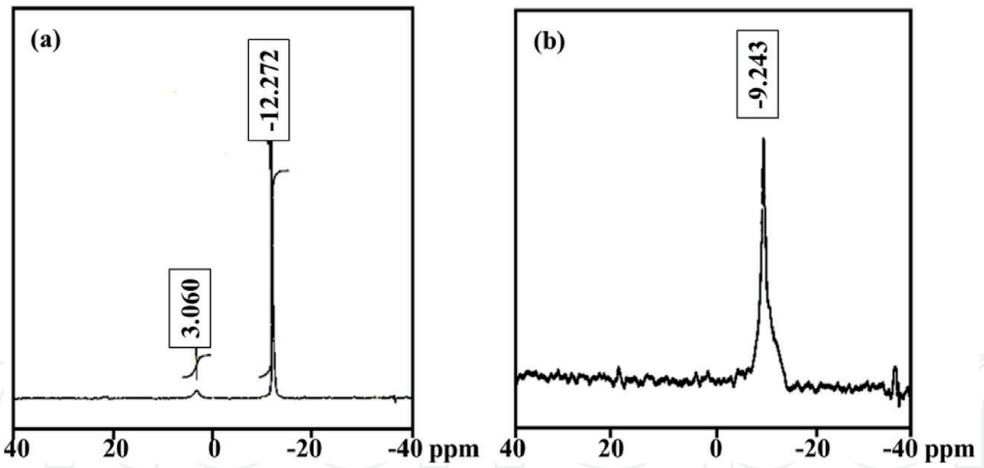

Figure 7.
^{31}P MAS NMR of (a) TPA-MCM-48 and (b) L-arg$_1$/TPA-MCM-48.

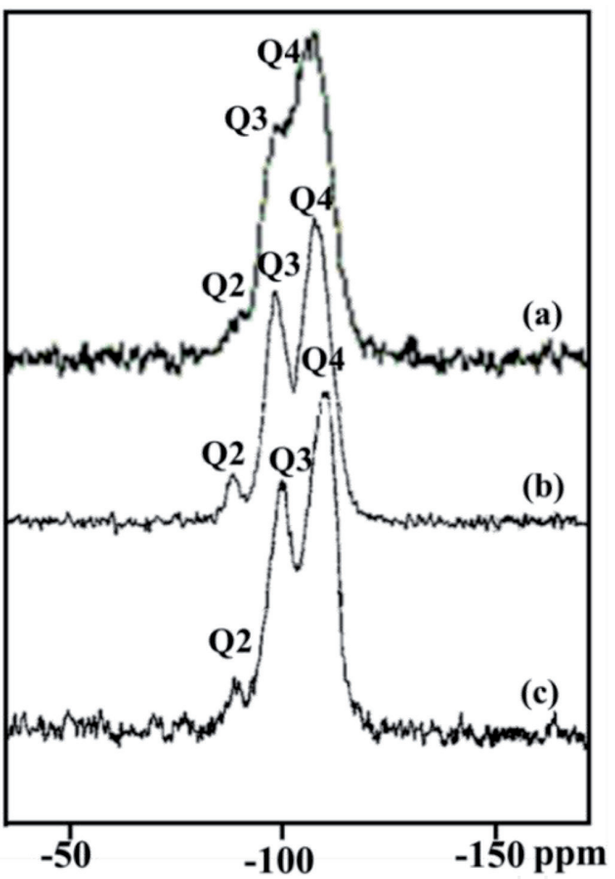

Figure 8.
(a) MCM-48, (b) TPA/MCM-48 and (c) L-arg$_1$/TPA-MCM-48.

All the three, Q2, Q3 and Q4 bands are observed in NMR spectra of TPA-MCM-48 (**Figure 8b**) suggesting the intact structure of MCM-48 even after functionalization. However, significant shift is observed in Q2 band from −92 to −88 (**Table 2**) suggests the interaction of Si-OH group of MCM-48 with TPA.

The ^{29}Si MAS NMR spectra of L-arg$_1$/TPA-MCM-48 show characteristic peaks (**Figure 8c**) of TPA-MCM-48 (**Table 2**). No significant shift in the Q2, Q3 and Q4 bands suggests that the structure of TPA-MCM-48 remains intact even after loading of L-arginine. This further confirms that the L-arginine molecules selectively bind with TPA and not to the surface Si-OH group of MCM-48.

Sr. No.	Materials	29Si MAS NMR data		
		Q2 ppm	Q3 ppm	Q4 ppm
1.	MCM-48	−92	−99	−108
2.	TPA-MCM-48	−88	−98	−108
3.	L-arg$_1$/TPA-MCM-48	−87	−98	−108

Table 2.
^{29}Si chemical shift of MCM-48, TPA-MCM-48 and L-arg1/TPA-MCM-48.

3.2 In vitro release study of L-arginine

3.2.1 Effect of stirring on release rate of L-arginine

In vitro release profile of L-arg$_1$/TPA-MCM-48 in SBF under static and stirring condition at 37°C was carried out and results are shown in **Figure 9**. Initially 28% of L-arginine is released under both the condition but after that more slower and delayed release is observed in case of static condition. It reached to 51 and 38% up to 10 h and 86 and 46% up to 32 h under stirring and static condition respectively. The slower release of L-arginine is may be due to the slow diffusion of L-arginine molecules under static condition.

As stated earlier all the experiments were carried out thrice. Statistics tool ANOVA was applied and the experimental errors within the data was found to be ±2%. The results of ANOVA single factor for release of L-arginine from TPA-MCM-48 under stirring and static condition are shown in **Table 3**. The calculated F values (0.339 under stirring and 3.062 under static conditions) are less than tabulated F value (3.09 under stirring and 3.097 under static conditions), and statistically significant difference (P) of 0.713 and 0.051 were obtained under stirring and static conditions respectively.

3.2.2 Effect of pH on release rate of L-arginine

To see the effect of pH on release rate of L-arginine, release study was carried out into SBF (pH 7.4) and SGF (pH 1.2) and results are compared (**Figure 10**). **Figure 10**. Shows slower release rate of L-arginine at lower pH. It is known that

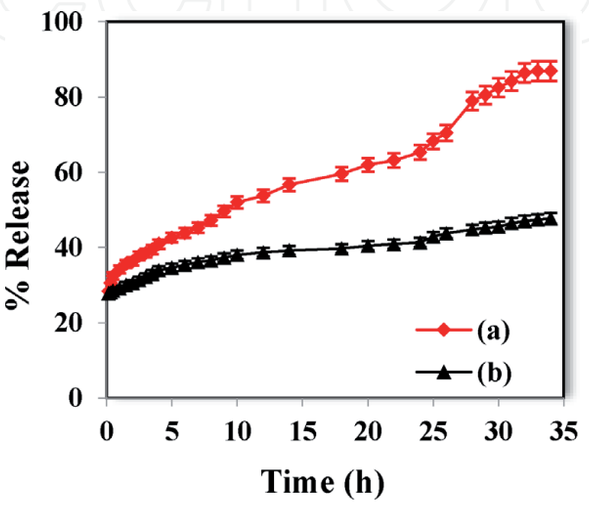

Figure 9.
In vitro release profile of L-arginine under (a) stirring condition and (b) static condition.

Condition	Source of variation	SS	df	MS	F	P-value	F crit
Stirring	Between groups	248	2	124	0.339	0.713	3.097
	Within groups	32878.21	90	365.31			
	Total	33126.21	92				
Static	Between groups	248	2	124	3.062	0.051	3.097
	Within groups	3644.169	90	40.49			
	Total	3892.169	92				

SS: sum of squares; Df: degree of freedom; MS: mean squares.

Table 3.
Results of ANOVA single factor.

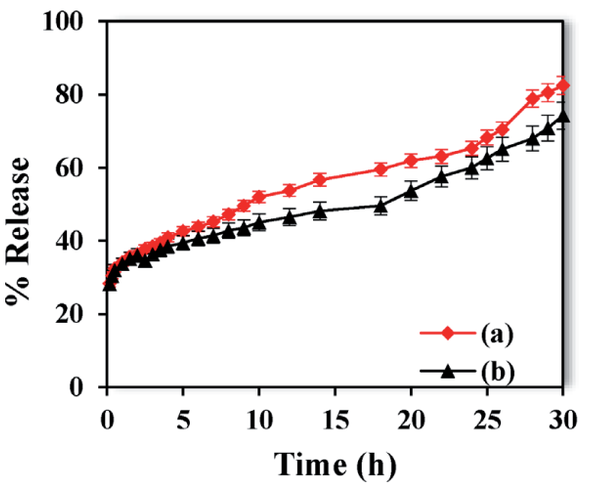

Figure 10.
In vitro release profile of L-arg1/TPA-MCM-48 in SBF (pH 7.4) and in SGF (pH 1.2).

Condition	Source of variation	SS	df	MS	F	P-value	F crit
In SBF (pH 7.4)	Between groups	248	2	124	0.339	0.713	3.097
	Within groups	32878.22	90	365.3136			
	Total	33126.22	92				
In SGF (pH 1.2)	Between groups	240.086	2	120.043	0.41457	0.661879	3.098
	Within groups	26060.44	90	289.5605			
	Total	26300.53	92				

SS: sum of squares; Df: degree of freedom; MS: mean squares.

Table 4.
Results of ANOVA single factor.

L-arginine acquires two positive charges at pH 1.2 becomes Arg^{2+} [60] which may have strong interaction with TPA-MCM-48. While at pH 7.4 it remain as Arg^{+} which may have comparatively weaker interaction with TPA-MCM-48 which allows easy diffusion of L-arginine at pH 7.4.

Under similar lines, ANOVA has also been applied for L-arginine release at different pH, and experimental error of ±2% within the data was obtained. From the results presented in **Table 4**, it can be seen that the calculated F values (0.339

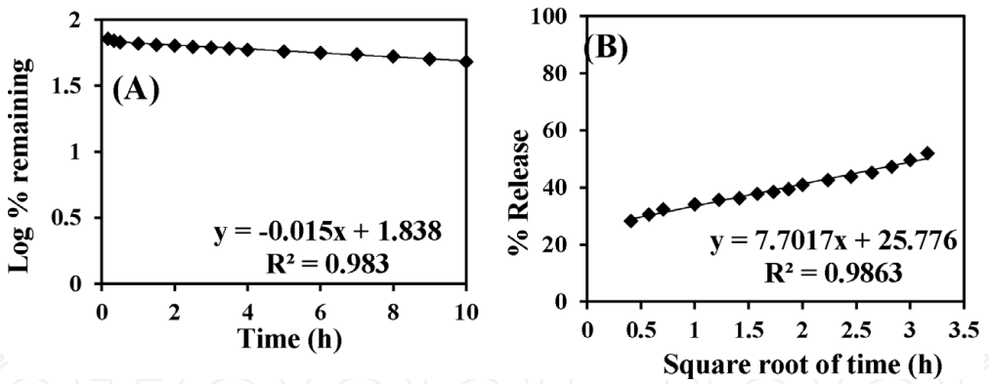

Figure 11.
(A) First order release kinetic model and (B) Higuchi model of L-arg$_1$/TPA-MCM-48.

at pH 7.4 and 0.414 at pH 1.2) are less than tabulated F value (3.09 at pH 7.4 and pH 1.2), and statistically significant difference (P) of 0.713 and 0.661 were obtained at pH 7.4 and 1.2 respectively.

3.2.3 Release kinetic and mechanism

For finding the drug release kinetic and mechanism released data up to 10 h were fitted with first order release kinetic model, Higuchi model and results are shown in **Figure 11** [61–63].

First order release kinetic model used to study the kinetic of release of soluble drugs. According to this model release of drug is concentration dependent process. **Figure 11A** shows first order release kinetic model of L-arg$_1$/TPA-MCM-48. The release of L-arginine follows the first order release kinetic model with higher linearity and co-relation coefficient (R^2 = 0.983).

Figure 11B Shows Higuchi model of L-arg$_1$/TPA-MCM-48 where % release of L-arginine was plotted against square root of time based on Fickian diffusion mechanism. According to this model release mechanism involves simultaneous penetration of SBF into the pores of carriers, dissolution of drug molecules and diffusion of these molecules from the carriers. This release data up to 10 h was best fitted with Higuchi model with higher linearity and co-relation coefficient (R^2 = 0.9863) and follows Fickian diffusion mechanism.

Hence release profile of L-arginine follows first order release kinetic model as well as Higuchi model.

3.2.4 Comparison of release profile of L-arginine from MCM-48 and TPA-MCM-48: role of TPA on release rate

To see the effect of TPA on release rate of L-arginine, release profile of L-arg$_1$/MCM-48 and L-arg$_1$/TPA-MCM-48 has been compared and results are shown in **Figure 12**. It is clear from the **Figure 12** that slower release profile is obtained for TPA-MCM-48 compared to pure MCM-48. In case of L-arg$_1$/MCM-48, initially 62% of L-arginine was released and reached to 76% up to 10 h. while in case of L-arg$_1$/TPA-MCM-48, initially 28% L-arginine released and reached to 51% up to 10 h. Thus, more controlled and ordered release rate is observed with TPA-MCM-48 systems compared to pure MCM-48. The slower release of L-arginine may be due to the strong interaction between L-arginine and terminal oxygen of TPA, which was already confirmed from FTIR spectra. Further, the pore volume of L-arg$_1$/MCM-48 is bigger than L-arg$_1$/TPA-MCM-48 (**Table 1**). So there may be easy diffusion of L-arginine molecules from MCM-48 compared to TPA-MCM-48. Here, TPA act as functionalizing agent and can hold the L-arginine for longer period of time.

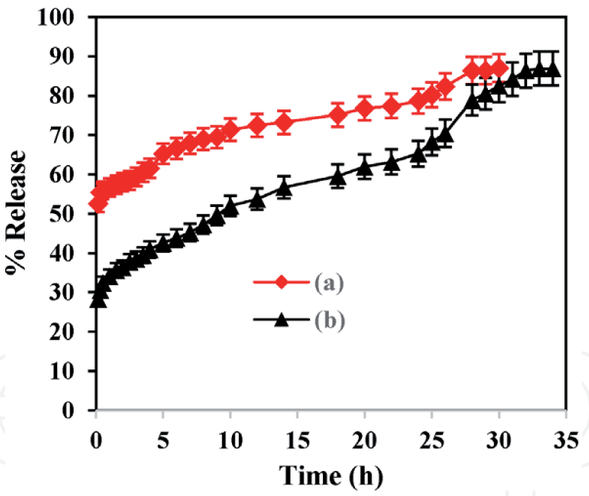

Figure 12.
Release profile of L-arg$_1$/MCM-48 and L-arg1/TPA-MCM-48.

Materials	Source of variation	SS	df	MS	F	P-value	F crit
L-arg/MCM-48	Between groups	216	2	108	1.449	0.240	3.113
	Within groups	5811.41	78	74.505			
	Total	6027.41	80				
L-arg/TPA-MCM-48	Between groups	248	2	124	0.339	0.713	3.0976
	Within groups	32878.22	90	365.3136			
	Total	33126.22	92				

SS: sum of squares; Df: degree of freedom; MS: mean squares.

Table 5.
Results of ANOVA single factor.

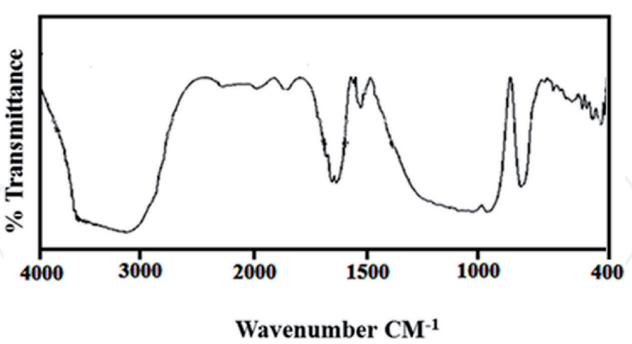

Figure 13.
FTIR spectrum of L-arg$_1$/TPA-MCM-48 after release study.

Under similar lines, ANOVA has also been applied for L-arginine release from MCM-48 as well as TPA-MCM-48, and experimental error of ±2% within the data was obtained. From the results presented in **Table 5**, it can be seen that the calculated F values (1.449 for L-arg$_1$/MCM-48 and 0.339 for L-arg$_1$/TPA-MCM-48) are lesser than tabulated F value (3.113 for L-arg/MCM-48 and 3.097 for L-arg/TPA-MCM-48), and statistically significant difference (P) of 0.240 and 0.713 were obtained for L-arg/MCM-48 and L-arg/TPA-MCM-48 respectively.

Further, to see that TPA is actually acting as functionalizing agent or not, FTIR analysis of L-arg$_1$/TPA-MCM-48 was carried out after release study and spectrum is shown in **Figure 13**. It shows that bands correspond to N-H stretching vibration

and CH_3 in plan bending vibration are disappeared. This may be due to the removal of L-arginine from TPA-MCM-48 during the release study. However the bands correspond to NH_2 in plan bending vibration and C=O stretching vibration show slight shifting with lower intensity. This suggests that some amount of L-arginine was remaining inside the TPA-MCM-48. That was also confirm from release study as it shows that 86% L-arginine was release up to 32 h and then it became constant. Further, bands corresponding to TPA-MCM-48 are remaining as it is and confirm the intact structure of TPA-MCM-48.

4. Conclusion

In this chapter first time we are reporting functionalization of MCM-48 using TPA and its application as carrier for L-arginine. FTIR and NMR studies shows that L-arginine interact with TPA-MCM-48 through its N-H and C=O group. Further, BET and TEM analysis shows that structure of MCM-48 remain intact even after functionalization as well as L-arginine loading. In vitro release studies suggest that more controlled and delayed release was obtained with TPA-MCM-48 system. Presence of TPA, delayed the release rate of L-arginine and this being of great importance in the field of controlled drug delivery system. Further kinetics and mechanism study shows that release of L-arginine follows first order kinetics with Fickian diffusion mechanism.

Acknowledgements

Authors are thankful to Department of Chemistry, Faculty of Science, The Maharaja Sayajirao University of Baroda for BET and TGA analysis.

Conflict of interest

The authors declare no conflict of interest.

DOI: http://dx.doi.org/10.5772/intechopen.90175

Author details

Anjali Uday Patel[1*] and Priyanka Dipakbhai Solanki[1,2]

1 Department of Chemistry, Faculty of Science, The Maharaja Sayajirao University of Baroda, Vadodara, Gujarat, India

2 Department of Education, Government Science College Dhanpur, Government of Gujarat, India

*Address all correspondence to: anjali.patel-chem@msubaroda.ac.in

References

[1] Rainer HB. The pharmacodynamics of L-arginine. The Journal of Nutrition. 2007;**137**:1650S-1655S. DOI: 10.1093/jn/137.6.1650S

[2] Karl IE, Klahr S, Reyes AA. Role of arginine in health and in renal disease. The American Journal of Physiology. 1994;**267**:F331-F346. DOI: 10.1152/ajprenal.1994.267.3.F331

[3] Morris SM. Arginine metabolism: Enzymology, nutrition and clinical significant. Journal of Nutrition. 2004;**134**:2743S-2747S

[4] Ann NY, Moncada S. Nitric oxide in the vasculature: Physiology and pathophysiology. Academy of Sciences. 1997;**811**:60-67. DOI: 10.1111/j.1749-6632.1997.tb51989.x

[5] Baylis C, Raij L. Glomerular actions of nitric oxide. Kidney International. 1995;**48**:20-32. DOI: 10.1038/ki.1995.262

[6] Cderbaum SD, Grody WW, Jenkinson CP. Comparative properties of arginases. Comparative Biochemistry and Physiology. Part B, Biochemistry and Molecular Biology. 1996;**114**:107-132

[7] Barbul A, Witte MB. Arginine physiology and its implication for wound healing. Wound Repair and Regeneration. 2003;**11**:419-423

[8] Marik PE, Siddiqui R, Terry C, Zaloga GP. Arginine: Mediator or modulator of sepsis? Nutrition in Clinical Practice. 2004;**19**:201-215. DOI: 10.1177/0115426504019003201

[9] Albina JE, Mills CD, Barbul A. Arginine metabolism in wounds. The American Journal of Physiology. 1988;**254**:E459-E467. DOI: 10.1152/ajpendo.1988.254.4.E459

[10] Childress B, Cowan L, Stechmiller JK.Arginine supplementation and wound healing. Nutrition in Clinical Practice. 2005;**20**:52-62. DOI: 10.1177/011542650502000152

[11] Blum A, Cannon RO, Csako G, Hathaway L, Kirby M, Mincemoyer R, et al. Oral l-arginine in patients with coronary artery disease on medical management. Circulation. 2000;**101**:2160-2164. DOI: 10.1161/01.cir.101.18.2160

[12] Fisher H, Sitren H. Nitrogen retention in rats fed on diets enriched with arginine and glycine: Improved N retention after trauma. The British Journal of Nutrition. 1977;**3**:195-208. DOI: 10.1079/bjn19770021

[13] Deng S, Dong S, Qiang G, Wanling S, Wujun X, XuYao W, et al. Amino acid adsorption on mesoporous materials: Influence of types of amino acids, modification of mesoporous materials, and solution conditions. The Journal of Physical Chemistry. B. 2008;**112**:261-2267. DOI: 10.1021/jp0763580

[14] (a)Vallet-Regi M, Balas F, Arcos D. Mesoporous materials for drug delivery. Angewandte Chemie, International Edition. 2007;**46**:7548-7558. DOI: 10.1002/anie.200604488.(b)Kmar T, Planin O. Ordered mesoporous silicates as matrices for controlled release of drugs. Acta Pharmaceutica. 2010;**60**:373-385. DOI: 10.2478/v1007-010-0037-4. (c)Manzanoab M, Vallet-Regi M. New developments in ordered mesoporous materials for drug delivery. Journal of Materials Chemistry. 2010;**20**:5593-5604. DOI: 10.1039/B922651F.(d)Yang P, Gaib S, Lin J. Functionalized mesoporous silica materials for controlled drug delivery. Chemical Society Reviews. 2012;**41**:3679-3698. DOI: 10.1039/C2CS15308D

[15] Tang Q, Chen Y, Chen J, Li J, Xu Y, Wub D, et al. Drug delivery from hydrophobic-modified mesoporous

silicas: Control via modification level and site-selective modification. Journal of Solid State Chemistry. 2010;**183**:76-83. DOI: 10.1016/j.jssc.2009.10.025

[16] Qua F, Zhua G, Lina H, Zhanga W, Suna J, Lia S, et al. A controlled release of ibuprofen by systematically tailoring the morphology of mesoporous silica materials. Journal of Solid State Chemistry. 2006;**179**:2027-2035. DOI: 10.1016/j.jssc.2006.04.002

[17] Yang P, Quan Z, Lu L, Huang S, Lin J, Fu H. Nanotechnology. 2007;**18**:235703-235715

[18] Yanga P, Quana Z, Lua L, Huanga S, Lin J. Luminescence functionalization of mesoporous silica with different morphologies and applications as drug delivery systems. Biomaterials. 2008;**29**:692-702. DOI: 10.1016/j.biomaterials.2007.10.019

[19] Lin G, Sun J, Li Z, Wang J, Ren B. Influence of different structured channels of mesoporous silicate on the controlled ibuprofen delivery. Materials Chemistry and Physics. 2012;**135**:786-797. DOI: 10.1016/j.matchemphys.2012.05.059

[20] Szegedi A, Popova M, Goshev I, Klébert S, Mihály J. Controlled drug release on amine functionalized spherical MCM-41. Journal of Solid State Chemistry. 2012;**194**:257-263. DOI: 10.1016/j.jssc.2012.05.030

[21] Kurczewska J, Lewandowski D, Olejnik A, Schroeder G, Nowak I. Double barrier as an effective method for slower delivery rate of ibuprofen. International Journal of Pharmaceutics. 2014;**472**:248-250. DOI: 10.1016/j.ijpharm.2014.06.037

[22] Qu F, Zhu G, Huang S, Li S, Qiu S. Effective controlled release of captopril by silylation of mesoporous MCM-41. ChemPhysChem. 2006;**7**:400-406. DOI: 10.1002/cphc.200500294

[23] Qu F, Zhu G, Huang S, Li S, Sun J. Controlled release of captopril by regulating the pore size and morphology of ordered mesoporous silica. Microporous and Mesoporous Materials. 2006;**92**:1-9. DOI: 10.1016/j.micromeso.2005.12.004

[24] Gai S, Yang P, Wang D, Li C, Niu N, He F, et al. Lin luminescence functionalization of MCM-48 by YVO4:Eu3+ for controlled drug delivery. Journal of RSC Advances. 2012;**2**:3281-3287. DOI: 10.1039/C2RA00862A

[25] Ambrogia V, Perioli L, Marmottinib F, Giovagnolia S, Espositoa M, Rossia C. Improvement of dissolution rate of piroxicam by inclusion into MCM-41 mesoporous silicate. European Journal of Pharmaceutical Sciences. 2007;**32**:216-222. DOI: 10.1016/j.ejps.2007.07.005

[26] Bernardos A, Aznar E, Coll C, Martínez-Mañez R, Barat JM, Marcos MD, et al. Controlled release of vitamin B2 using mesoporous materials functionalized with amine-bearing gate-like scaffoldings. Journal of Controlled Release. 2008;**131**:181-189. DOI: 10.1016/j.jconrel.2008.07.037

[27] Ambrogi V, Perioli L, Marmottini F, Moretti M, Lollini E, Rossi C. Chlorhexidine MCM-41 mucoadhesive tablets for topical use. Journal of Pharmaceutical Innovation. 2009;**4**:156-164. DOI: 10.1007/s12247-009-9073-3

[28] Vafaee M, Amini MM, Najafi F, Sadeghi O, Amani V. Modified nanoporous silicas for oral delivery of the water insoluble organotin compound: Loading and release of methylphenyltin dichloride as an anti-tumor drug model. Journal of Sol-Gel Science and Technology. 2012;**64**:411-417

[29] Maria G, Stoica A-I, Luta I, Stirbet D, Radu GL. Cephalosporin

release from functionalized MCM-41 supports interpreted by various models. Microporous and Mesoporous Materials. 2012;**162**:80-90. DOI: 10.1016/j.micromeso.2012.06.013

[30] Nastase S, Bajenaru L, Berger D, Matei C, Moisescu MG, Constantin D, et al. Mesostructured silica matrix for irinotecan delivery systems. Central European Journal of Chemistry. 2014;**12**:813-820

[31] Areana CO, Vesgaa MJ, Parrab JB, Delgado MR. Effect of amine and carboxyl functionalization of sub-micrometric MCM-41 spheres on controlled release of cisplatin. Ceramics International. 2013;**39**:7407-7414. DOI: 10.1016/j.ceramint.2013.02.084

[32] Wang Y, Sun L, Jiang T, Zhang J, Zhang C, Sun C, et al. The investigation of MCM-48-type and MCM-41-type mesoporous silica as oral solid dispersion carriers for water insoluble cilostazol. Drug Development and Industrial Pharmacy. 2013;**40**(6):819-828. DOI: 10.3109/03639045.2013.788013

[33] Kiwilsza A, Milanowski B, Druzbicki K, Coy LE, Grzeszkowiak M, Jarek M, et al. Mesoporous drug carrier systems for enhanced delivery rateof poorly water-soluble drug: Nimodipine. Journal of Porous Materials. 2015;**22**:817-829. DOI: 10.1007/s10934-015-9955-3

[34] Liu X, Che S. CFD investigation and PIV validation of flow field in a compact return diffuser under strong part-load conditions. Science China Chemistry. 2015;**58**:400-410. DOI: 10.1007/s11431-014-5743-6

[35] Nairi V, Medda L, Monduzzi M, Salis A. Adsorption and release of ampicillin antibiotic from ordered mesoporous silica. Journal of Colloid and Interface Science. 2017;**497**:217-225. DOI: 10.1016/j.jcis.2017.03.021

[36] Cuelloa NI, Elíasa VR, Mendieta SN, Longhi M, Crivelloa ME, Olivac MI, et al. Drug release profiles of modified MCM-41 with superparamagnetic behavior correlated with the employed synthesis method. Materials Science and Engineering: C. 2017;**78**:674-681. DOI: 10.1016/j.msec.2017.02.010

[37] Nastase S, Bajenaru L, Matei C, Mitran RA, Berger D. Ordered mesoporous silica and aluminosilicate-type matrix for amikacin delivery systems. Microporous and Mesoporous Materials. 2013;**182**:32-39. DOI: 10.1016/j.micromeso.2013.08.018

[38] Jesus RA, Rabelo AS, Figueiredo RT, Cides da Silva LC, Codentino IC, Fantini MCA, et al. Synthesis and application of the MCM-41 and SBA-15 as matrices for in vitro efavirenz release study. Journal of Drug Delivery Science and Technology. 2016;**31**:153-159. DOI: 10.1016/j.jddst.2015.11.008

[39] Berger D, Bajenaru L, Nastase S, Mitran R-A, Munteanu C, Matei C.Influence of structural, textural and surface properties of mesostructured silica and aluminosilicate carriers on aminoglycoside uptake and in vitro delivery. Microporous and Mesoporous Materials. 2015;**206**:150-160. DOI: 10.1016/j.micromeso.2014.12.022

[40] Arruebo M, Galan M, Navascues N, Tellez C, Marquina C, Ibarra MR. Santamari development of magnetic nanostructured silica-based materials as potential vectors for drug-delivery applications. Chemistry of Materials. 2006;**18**:1911-1919. DOI: 10.1021/cm051646z

[41] Yang P, Yang P, Teng X, Linb J, Huang L. A novel luminescent mesoporous silica/apatite composite for controlled drug release. Journal of Materials Chemistry. 2011;**21**:5505-5510. DOI: 10.1039/C0JM03878D

[42] Gai S, Yang P, Wang D, Li C, Niu N, He F, et al. Luminescence functionalization of MCM-48 by YVO4:Eu3+ for controlled drug delivery. Journal of RSC Advances. 2012;**2**:3281-3287. DOI: 10.1039/C2RA00862A

[43] Aghaei H, Nourbakhsh AA, Karbasi S, Kalbasi RJ, Rafienia M, Nourbakhsh N, et al. Investigation on bioactivity and cytotoxicity of mesoporous nano-composite MCM-48/hydroxyapatite for ibuprofen drug delivery. Ceramics International. 2014;**40**:7355-7362

[44] Popat A, Jambhrunkar S, Zhang J, Yang J, Zhang H, Meka A, et al. Programmable drug release using bioresponsive mesoporous silica nanoparticles for site-specific oral drug delivery. Chemical Communications. 2014;**50**:5547-5550. DOI: 10.1039/C4CC00620H

[45] Choi E, Lu J, Tamanoi F, Zink JI. Drug release from three-dimensional cubic mesoporous silica nanoparticles controlled by nanoimpellers. Zeitschrift für Anorganische und Allgemeine Chemie. 2014;**640**:3-4. 588-594. DOI: 10.1002/zaac.201300503

[46] Tanga Q, Xu Y, Wu D, Sun Y. Journal of Solid State Chemistry. 2006;**179**:1513-1520

[47] Hill CL, Weeks JMS, Schinazi RF. Anti-HIV-1 activity, toxicity, and stability studies of representative structural families of polyoxometalates. Journal of Medicinal Chemistry. 1990;**33**:2767-2772. DOI: 10.1021/jm00172a014

[48] Weeks MS, Hill CL, Schinazi RF. Synthesis, characterization, and anti-human immunodeficiency virus activity of water-soluble salts of polyoxotungstate anions with covalently attached organic groups. Journal of Medicinal Chemistry. 1992;**35**:1216-1221. DOI: 10.1021/jm00085a008

[49] Judd DA, Nettles JH, Nevins N, Snyder JP, Liotta DC, Tang J, et al. Polyoxometalate HIV-1 protease inhibitors. A new mode of protease inhibition. Journal of the American Chemical Society. 2001;**123**:886-897. DOI: 10.1021/ja001809e

[50] Xia L, Wang S, Feng C. Synthesis and anticancer properties of tungstosilicic polyoxometalate containing 5-fluorouracil and neodymium. Journal of Rare Earths. 2010;**28**:965-968. DOI: 10.1016/S1002-0721(09)60227-1

[51] Nomiya K, Torii H, Hasegawa T, Nemoto Y, Nomura K, Hashino K, et al. Insulin mimetic effect of a tungstate cluster. Effect of oral administration of homo-polyoxotungstates and vanadium-substituted polyoxotungstates on blood glucose level of STZ mice. Journal of Inorganic Biochemistry. 2001;**86**:657-667. DOI: 10.1016/S0162-0134(01)00233-1

[52] Yamamuro TJ. Solutions able to reproduce in vivo surface-structure changes in bioactive glass-ceramic A-W^3. Biomedical Materials Research. 1990;**24**:721

[53] Kumar D, Schumacher K, Hohenesche CDFV, Grun M, Unger KK. MCM-41, MCM-48 and related mesoporous adsorbents: Their synthesis and characterization. Colloids and Surfaces A: Physicochemical and Engineering Aspects. 2001, 2001;**109-116**:187-188. DOI: 10.1016/S0927-7757(01)00638-0

[54] Singh S, Patel A. 12-Tungsto-phosphoric acid supported on mesoporous molecular material: Synthesis, characterization and performance in biodiesel production. Journal of Cleaner Production. 2014;**72**:46-56. DOI: 10.1016/j.jclepro.2014.02.057

[55] Yijun Z, Shuijin Y. Synthesis, characterization and catalytic

application of H3PW12O40/MCM-48 in the esterification of methacrylic acid with n-butyl alcohol. Journal Wuhan University of Technology, Materials Science Edition. 2008;**23**:346-349. DOI: 10.1007/s11595-007-3346-9

[56] Kozhevnikov IV, Kloetstra KR, Sinnema A, Zandbergen HW, Bekkum HV. Study of catalysts comprising heteropoly acid $H_3PW_{12}O_{40}$ supported on MCM-41 molecular sieve and amorphous silica. Journal of Molecular Catalysis A: Chemical. 1996;**114**:287-298. DOI: 10.1016/S1381-1169(96)00328-7

[57] Kumar S, Rai SB. Spectroscopic studies of L-arginine molecule. Indian Journal of Pure and Applied Physics. 2010;**48**:251-255. Available from: http://nopr.niscair.res.in/handle/123456789/7643

[58] Okuhara T, Mizuno N, Misono M. Catalytic chemistry of heteropoly compounds. Advances in Catalysis. 1994;**41**:113-252. DOI: 10.1016/S0360-0564(08)60041-3

[59] Mizuno N, Misono M. Pore structure and surface area of $Cs_xH3_xPMo_{12}O_{40}$ (x ¼ 0e3, M ¼ W, Mo). Chemistry Letters. 1987;**16**:967-970

[60] Qiang G, Wujun X, Yao X, Dong W, Yuhan S, Deng F, et al. Interactions of lipid bilayers with supports: A coarse-grained molecular simulation study. The Journal of Physical Chemistry B. 2008;**112**:261-2267. DOI: 10.1021/jp077305l

[61] Costa P, Sousa Lobo JM. Modeling and comparison of dissolution profiles. European Journal of Pharmaceutical Sciences. 2001;**13**:123-133. DOI: 10.1016/S0928-0987(01)00095-1

[62] Singhvi G, Singh M. Review: In-vitro drug release characterization models. International Journal of Pharmaceutical Studies and Research. 2011;**2**(1):77-84

[63] Salome C, Godswill O, Ikechukwu O.Kinetics and mechanisms of drug release from swellable and non swellable matrices: A review. Research Journal of Pharmaceutical, Biological and Chemical Sciences. 2013;**4**:2,97-2,2103